Wave propagation in a duct with a periodic Helmholtz resonators array

Xu Wang and Cheuk-Ming Mak[a)]
Department of Building Services Engineering, The Hong Kong Polytechnic University, Hung Hom, Kowloon, Hong Kong, China

(Received 10 June 2011; revised 21 November 2011; accepted 29 November 2011)

Helmholtz resonator is often used to reduce noise in a narrow frequency range. To obtain a broader noise attenuation band, combing several resonators is a possible way. This paper presents a theoretical study of sound propagation in a one-dimensional duct with identical side-branch resonators mounted periodically. The analysis of each resonator was based on a distributed-parameter model that considered multi-dimensional wave propagation in its neck-cavity interface. This model provided a more accurate prediction of the resonant frequency of the resonator than traditional lumped-parameter model. Bloch wave theory and the transfer matrix method were used to investigate wave propagation in these spatially periodic resonators. The results predicted by the theory fit well with the computer simulation using a three-dimensional finite element method and the experimental results. This study indicates that the wave coupling in this periodic system results in the dispersion of the frequency band into the stop and the pass bands. The long-term significance is that periodic resonators may more effectively control noise in ducts by broadening the bandwidth they attenuate and increasing the magnitude of sound attenuation. © *2012 Acoustical Society of America*.
[DOI: 10.1121/1.3672692]

PACS number(s): 43.50.Gf, 43.20.Mv [BSC] Pages: 1172–1182

I. INTRODUCTION

A periodic structure is composed of a number of identical structural components that are joined together end-to-end and/or side-by-side to form a whole complex.[1] Periodic structures can be classified into three categories: (1) the periodic medium, (2) the periodically inhomogeneous medium, and (3) the periodically bounded medium.[2] The study of Rayleigh[3] on wave propagation in a stretched string with periodic density is an example of the first class of periodic structures, i.e., the periodic medium. Related work can be found on structure-borne sound, in particular, on sound propagation in one-, two-, and three-dimensional periodic structures, such as beams,[4,5] plates,[6,7] and shells[8,9] in various combinations and support conditions, or even with multiple layers.[10] An example of the second class is a fluid having a periodic variation in ambient density or sound speed.[2] The work involving periodically inhomogeneous media is about the quantum theory of electrical conductivity.[11] The third class of periodic structures is a system composed of a homogeneous medium with a periodically vary boundary. Related work can be found on airborne sound, in particular, on sound propagation in a duct with periodically varying cross section,[12] a duct loaded periodically with quarter-wavelength tubes,[2] or a duct with periodic arrays of obstacles inside.[13] The duct loaded periodically with Helmholtz resonators, which is found to be a new class of ultrasonic metamaterials that have a negative modulus near the resonance frequency,[14] is the subject of present study.

Helmholtz resonators (called simply resonators, hereafter) are devices with a resonance peak designed to control noise. They are useful against noise centralized in a narrow frequency band. Many studies have tried to accurately predict resonant frequency. Initially, Rayleigh treated resonators as lumped-parameter systems[15] in which the air in the neck acts as mass and the air inside its cavity acts as a spring. Tang and Sirignano[16] derived a general model that considers one-dimensional wave propagation inside both the neck and cavity. This model was then expanded by Monkewitz *et al.*[17] and Selamet *et al.*[18,19] Their studies investigated two- and three-dimensional wave propagations in resonators. Their models fit their experimental results better than the lumped-parameter model.[15]

Because a single resonator has a narrow resonance peak, combining several resonators is a possible way to obtain a broader band of noise attenuation. An array of differently tuned resonators was used in some previous works to decrease broadband noise.[20–22] The duct with multiple similar resonators that includes a duct with the boundary of a perforated or micro-perforated plate backed by air cavities, was discussed.[22–24] It is found that when resonators of similar resonance frequency are in close proximity, they can interact and lead to a decrease in the overall performance compared to that of a single resonator.[24] To avoid this interaction, the resonators at some distance between each other were considered in most of the works.[22,23] However, to investigate the unusual attenuation of sound transmission in the periodic structure at low to medium frequencies, the distance between two nearby resonators should be larger. In the present study, this distance between two nearby resonators is much larger than the dimension of the resonators. It is hoped that the present study can provide a stepping stone for investigation of the acoustic properties of ducts loaded periodically with resonators and its potential application in noise control.

[a)]Author to whom correspondence should be addressed. Electronic mail: becmmak@polyu.edu.hk

II. THE DISTRIBUTED-PARAMETER MODEL OF RESONATORS

This study considers only circular concentric resonators. As shown in Fig. 1, a resonator, with neck/cavity radius r_1/r_2, cross sectional area S_1/S_2 and length l_1/l_2, respectively, is mounted on a duct with cross sectional area S_d as a side branch. Interested readers can find a detailed discussion of the distributed-parameter model of resonators in Ref. 19. However, for the sake of completeness, a brief description of this model is required here. And it is rewritten here in terms of matrices.

The sound pressure in the neck (P_1) and cavity (P_2) can be expressed as[19,25,28]

$$P_q(r,z_q)=A_0^{(q)}e^{-jkz_q}+\sum_{n=1}^{+\infty}A_n^{(q)}J_0(k_{r,n}^{(q)}r)e^{-jk_{z,n}^{(q)}z_q}+B_0^{(q)}e^{jkz_q}+\sum_{n=1}^{+\infty}B_n^{(q)}J_0(k_{r,n}^{(q)}r)e^{jk_{z,n}^{(q)}z_q},\quad q=1,2 \tag{1}$$

in a cylindrical coordinate as the combination of inward-going planar waves (the first term), radial waves (the second term), outward-going planar waves (the third term), and radial waves (the fourth term), where the subscript or superscript $q=1$ indicates that it is a parameter considered in the neck of the resonator; the subscript or superscript $q=2$ indicates that it is a parameter considered in the cavity of the resonator. Herein $A_0^{(q)}$, $A_n^{(q)}$, $B_0^{(q)}$, and $B_n^{(q)}$ are the complex constants related to the magnitude of the corresponding wave mode. J_0 is the Bessel function of first kind and order zero.[26] k, $k_{r,n}^{(q)}$, and $k_{z,n}^{(q)}$ represent the wave number, the radial wave number of mode n, and the axial wave number of mode n (respectively), with the relation $k^2=(k_{r,n}^{(q)})^2+(k_{z,n}^{(q)})^2 (q=1,2)$. In terms of the momentum equation, the particle velocity in z-direction can be obtained as

$$V_q(r,z_q)=\frac{A_0^{(q)}}{\rho c}e^{-jkz_q}+\frac{1}{\rho\omega}\sum_{n=1}^{+\infty}A_n^{(q)}k_{z,n}^{(q)}J_0(k_{r,n}^{(q)}r)e^{-jk_{z,n}^{(q)}z_q}-\frac{B_0^{(q)}}{\rho c}e^{jkz_q}-\frac{1}{\rho\omega}\sum_{n=1}^{+\infty}B_n^{(q)}k_{z,n}^{(q)}J_0(k_{r,n}^{(q)}r)e^{jk_{z,n}^{(q)}z_q},\quad q=1,2 \tag{2}$$

where ρ is the air density, c is the speed of sound, and ω is the circular frequency. The wall of the resonator is assumed to be rigid without any absorption materials, so the boundary conditions

$$\left.\frac{\partial P_1(r,z_1)}{\partial r}\right|_{r=r_1}=0,\left.\frac{\partial P_2(r,z_2)}{\partial r}\right|_{r=r_2}=0,\left.\frac{\partial P_2(r,z_2)}{\partial z_2}\right|_{z_2=l_2}=0 \tag{3}$$

give

$$k_{r,n}^{(1)}=\chi_n/r_1,\quad k_{r,n}^{(2)}=\chi_n/r_2 \tag{4}$$

and

$$B_0^{(2)}e^{jkl_2}=A_0^{(2)}e^{-jkl_2},\quad B_n^{(2)}e^{jk_{z,n}^{(2)}l_2}=A_n^{(2)}e^{-jk_{z,n}^{(2)}l_2} \tag{5}$$

where χ_n is the nth root of the function[26] $J_0'(\chi_n)=0$.

At the neck-cavity interface of the resonator, the continuity conditions of sound pressure and particle velocity

$$P_1(r,z_1)|_{z_1=l_1}=P_2(r,z_2)|_{z_2=0},\quad 0\le r\le r_1, \tag{6}$$

$$V_1(r,z_1)|_{z_1=l_1}=V_2(r,z_2)|_{z_2=0},\quad 0\le r\le r_1 \tag{7}$$

give

$$\frac{1}{2}r_1^2(A_0^{(1)}e^{-jkl_1}+B_0^{(1)}e^{jkl_1})=\frac{1}{2}r_1^2(A_0^{(2)}+B_0^{(2)})+\sum_{n=1}^{+\infty}(A_n^{(2)}+B_n^{(2)})\frac{r_1r_2}{\chi_n}J_1\left(\frac{r_1}{r_2}\chi_n\right), \tag{8}$$

$$\frac{1}{2}r_1^2[J_0(\chi_m)]^2(A_m^{(1)}e^{-jk_{z,m}^{(1)}l_1}+B_m^{(1)}e^{jk_{z,m}^{(1)}l_1})=\sum_{n=1}^{+\infty}(A_n^{(2)}+B_n^{(2)})\frac{r_1}{\left(\frac{x_n}{r_2}\right)^2-\left(\frac{x_m}{r_1}\right)^2}\frac{\chi_n}{r_2}J_0(\chi_m)J_1\left(\frac{r_1}{r_2}\chi_n\right) \tag{9}$$

and

$$r_1^2(A_0^{(1)}e^{-jkl_1}-B_0^{(1)}e^{jkl_1})=r_2^2(A_0^{(2)}-B_0^{(2)}), \tag{10}$$

$$\frac{1}{2}r_2^2k_{z,m}^{(2)}[J_0(\chi_m)]^2(A_m^{(2)}-B_m^{(2)})-k(A_0^{(1)}e^{-jkl_1}-B_0^{(1)}e^{jkl_1})\times\frac{r_1r_2}{\chi_m}J_1\left(\frac{r_1}{r_2}\chi_m\right)=\sum_{n=1}^{+\infty}k_{z,n}^{(1)}\left(A_n^{(1)}e^{-jk_{z,n}^{(1)}l_1}-B_n^{(1)}e^{jk_{z,n}^{(1)}l_1}\right)\times\frac{r_1}{\left(\frac{\chi_m}{r_2}\right)^2-\left(\frac{\chi_n}{r_1}\right)^2}\frac{\chi_m}{r_2}J_0(\chi_n)J_1\left(\frac{r_1}{r_2}\chi_m\right) \tag{11}$$

where J_1 is the Bessel function of first kind and order one,[26] and $m=1,2,\ldots,+\infty$ in both Eqs. (9) and (11).

The frequency range concerned in the present study is well below the cut-on frequency of the resonator neck and the duct. It means that the nonplanar waves excited at the discontinuity junction (the duct-neck interface) will decay exponentially. Therefore, only planar waves are assumed to exist in the duct-neck interface. This is an approximation, which helps us to develop a direct relation of the sound pressure in the duct and neck by ignoring the multi-dimension

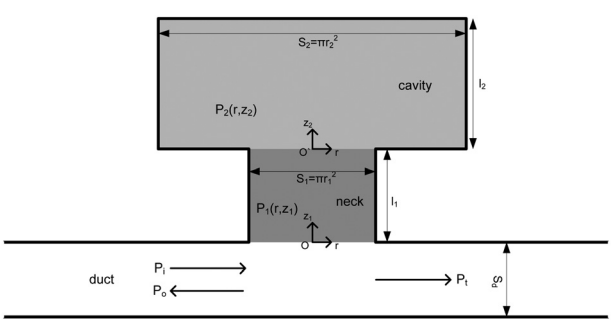

FIG. 1. Side-branch Helmholtz resonator.

effect in this complex interface. Due to this assumption, $A_n^{(1)}$ is set to zero. At the meantime, nonplanar waves can also be excited at the neck-cavity interface due to the sudden area discontinuity. This multi-dimension effect can no longer be ignored since it can be considered as sounds radiate into a bigger space (cavity) and the frequency may not below the cut-on frequency of the cavity. However, the nonplanar waves excited at the neck-cavity interface traveling in the neck in negative-z direction will decay over the length of the neck (i.e., $k_{z,n}^{(1)}$ should be imaginary). In this case, P_1 is assumed to be one-dimensional in the duct-neck interface and two-dimensional in the neck-cavity interface. So P_1 is no longer a variation of r in the vicinity of $z_1 = 0$. At the duct-neck interface, the continuity conditions of sound pressure and volume velocity can be expressed as

$$P_i + P_o = P_1|_{z_1=0} = P_t, \tag{12}$$

$$\frac{P_i - P_o}{\rho c} S_d = V_1|_{z_1=0} S_1 + \frac{P_t}{\rho c} S_d \tag{13}$$

which give

$$S_d P_i = (S_d + 0.5S_1)A_0^{(1)} + (S_d - 0.5S_1)B_0^{(1)}. \tag{14}$$

Combining Eqs. (5), (8)–(11), and (14) yields an equation set that determines the complex coefficients $A_0^{(1)}$, $B_0^{(1)}$, $B_n^{(1)}$, $A_0^{(2)}$, $B_0^{(2)}$, $A_n^{(2)}$, and $B_n^{(2)}$. Since higher-order harmonic components have a diminishing effect on the solution,[19,27] we can use a finite number of terms instead of an infinite summation of all modes and still ensure that the solution is reasonably accurate. Assuming that P_1/P_2 is made of harmonic components up to order N/M, respectively, the equation set can then be rewritten in terms of matrices, as

$$\mathbf{U}\mathbf{x} = \mathbf{y} \text{ or } \mathbf{x} = \mathbf{U}\backslash\mathbf{y}, \tag{15}$$

where $\mathbf{x}$ and $\mathbf{y}$ are both $(4+N+2M)$-dimensional vectors, which are given by

$$\mathbf{x} = \begin{bmatrix} A_0^{(1)} & B_0^{(1)} & B_1^{(1)} & \cdots & B_N^{(1)} & A_0^{(2)} & B_0^{(2)} & A_1^{(2)} & B_1^{(2)} & \cdots & A_M^{(2)} & B_M^{(2)} \end{bmatrix}^T, \tag{16}$$

$$\mathbf{y} = \begin{bmatrix} S_d P_i & 0_{1\times(3+N+2M)} \end{bmatrix}^T. \tag{17}$$

And $\mathbf{U}$ is a square matrix of dimension $(4+N+2M) \times (4+N+2M)$, which can be written as $\mathbf{U} = [\mathbf{U}_1 \quad \mathbf{U}_2 \quad \mathbf{U}_3 \quad \mathbf{U}_4]^T$. Herein the $3 \times (4+N+2M)$-dimensional matrix $\mathbf{U}_1$ is given by

$$\mathbf{U}_1 = \begin{bmatrix} S_d + 0.5S_1 & S_d - 0.5S_1 & \mathbf{0}_{1\times N} & & \mathbf{0}_{1\times(2+2M)} & \\ r_1^2 e^{-jkl_1} & -r_1^2 e^{jkl_1} & \mathbf{0}_{1\times N} & -r_2^2 & r_2^2 & \mathbf{0}_{1\times 2M} \\ r_1^2 e^{-jkl_1} & r_1^2 e^{jkl_1} & \mathbf{0}_{1\times N} & -r_1^2 & -r_1^2 & \mathbf{C}_{1\times 2M} \end{bmatrix} \tag{18}$$

where $\mathbf{0}$ denotes a zero matrix, with the subscript such as $1 \times N$ indicating its dimension, and

$$\mathbf{C}_{1\times 2M} = -2r_1 r_2 \left[\frac{1}{\chi_1} J_1\left(\frac{r_1}{r_2}\chi_1\right) \quad \frac{1}{\chi_1} J_1\left(\frac{r_1}{r_2}\chi_1\right) \quad \cdots \quad \frac{1}{\chi_M} J_1\left(\frac{r_1}{r_2}\chi_M\right) \quad \frac{1}{\chi_M} J_1\left(\frac{r_1}{r_2}\chi_M\right) \right]. \tag{19}$$

$\mathbf{U}_2$ is a $(M+1) \times (4+N+2M)$ matrix, as $\mathbf{U}_2 = \begin{bmatrix} \mathbf{0}_{(M+1)\times(N+2)} & \mathbf{D}_{(M+1)\times(2+2M)} \end{bmatrix}$, where

$$\mathbf{D}_{(M+1)\times(2+2M)} = \begin{bmatrix} e^{-jkl_2} & -e^{jkl_2} & & & \cdots & 0 \\ & & e^{-jk_{z,1}^{(2)} l_2} & -e^{jk_{z,1}^{(2)} l_2} & & \\ \vdots & & & & \ddots \quad \ddots & \vdots \\ 0 & & \cdots & & e^{-jk_{z,M}^{(2)} l_2} & -e^{jk_{z,M}^{(2)} l_2} \end{bmatrix}. \tag{20}$$

The $N \times (4+N+2M)$-dimensional matrix $\mathbf{U}_3$ is given by $\mathbf{U}_3 = [\mathbf{0}_{N\times 2} \quad \mathbf{E}_{N\times N} \quad \mathbf{0}_{N\times 2} \quad \mathbf{F}_{N\times 2M}]$, in which

$$\mathbf{E}_{N\times N} = \frac{1}{2} r_1^2 \begin{bmatrix} [J_0(\chi_1)]^2 e^{jk_{z,1}^{(1)} l_1} & & \\ & \ddots & \\ & & [J_0(\chi_N)]^2 e^{jk_{z,N}^{(1)} l_1} \end{bmatrix}, \tag{21}$$

$$\mathbf{F}_{N\times 2M} = \frac{r_1}{r_2}\begin{bmatrix} \Psi_{1,1} & \cdots & \Psi_{M,1} \\ \vdots & \ddots & \vdots \\ \Psi_{1,N} & \cdots & \Psi_{M,N} \end{bmatrix} \times \begin{bmatrix} 1 & 1 & & & \\ & & \ddots & \ddots & \\ & & & & 1 \quad 1 \end{bmatrix} \tag{22}$$

where

$$\Psi_{m,n} = \frac{\chi_m}{\left(\frac{\chi_m}{r_2}\right)^2 - \left(\frac{\chi_n}{r_1}\right)^2} J_0(\chi_n) J_1\left(\frac{r_1}{r_2}\chi_m\right),$$
$$n = 1, 2, \ldots N \text{ and } m = 1, 2, \ldots, M.$$

$\mathbf{U}_4$ is a $M \times (4 + N + 2M)$ matrix, as $\mathbf{U}_4 = [\mathbf{I}_{M\times 2} \quad \mathbf{J}_{M\times N} \quad \mathbf{0}_{N\times 2} \quad \mathbf{K}_{M\times 2M}]$, in which

$$\mathbf{I}_{M\times 2} = -kr_1r_2\begin{bmatrix} \frac{J_1\left(\frac{r_1}{r_2}\chi_1\right)}{\chi_1} \\ \vdots \\ \frac{J_1\left(\frac{r_1}{r_2}\chi_M\right)}{\chi_M} \end{bmatrix} \times \begin{bmatrix} e^{-jkl_1} & -e^{jkl_1} \end{bmatrix}, \tag{23}$$

$$\mathbf{J}_{\mathbf{M}\times\mathbf{N}} = \frac{r_1}{r_2}\begin{bmatrix} k_{z,1}^{(1)}\Psi_{1,1}e^{jk_{z,1}^{(1)}l_1} & \cdots & k_{z,N}^{(1)}\Psi_{1,N}e^{jk_{z,1}^{(1)}l_1} \\ \vdots & & \vdots \\ k_{z,1}^{(1)}\Psi_{M,1}e^{jk_{z,1}^{(1)}l_1} & \cdots & k_{z,N}^{(1)}\Psi_{M,N}e^{jk_{z,1}^{(1)}l_1} \end{bmatrix}, \tag{24}$$

$$\mathbf{K}_{M\times 2M} = \frac{1}{2}r_2^2\begin{bmatrix} [J_0(\chi_1)]^2 k_{z,1}^{(2)} & & \\ & \ddots & \\ & & [J_0(\chi_M)]^2 k_{z,M}^{(2)} \end{bmatrix} \times \begin{bmatrix} 1 & -1 & & & \\ & & \ddots & \ddots & \\ & & & & 1 \quad -1 \end{bmatrix}. \tag{25}$$

III. WAVE PROPAGATION IN A SEMI-INFINITE DUCT LOADED PERIODICALLY WITH RESONATORS

A. Theoretical outline

This section considers a semi-infinite duct loaded periodically with resonators, as shown in Fig. 2. Compared with the length of duct segment between two nearby resonators D, the diameter of the neck of the resonator is assumed to be negligible. In other words, D also can be regarded as the periodic distance.

As shown in Fig. 2, a typical periodic cell consists of the duct segment and a resonator attached to the left. As assumed in Sec. II, only planar waves exist in the duct and the vicinity of the opening of the resonator. In the region of the nth periodic element ($(n-1)D \le x \le nD$), the sound traveling in positive- and negative-x directions can be described with sound pressure $P_n^+(x) = C_n^+ e^{-jk(x-(n-1)D)}$ and $P_n^-(x) = C_n^- e^{jk(x-(n-1)D)}$, where C_n^+ and C_n^- are complex constants related to the magnitude of positive- and negative-going planar waves in the nth duct segment respectively. In the region of the next cell ($nD \le x \le (n+1)D$), the acoustic field has a similar form, with sound pressure $P_{n+1}^+(x) = C_{n+1}^+ e^{-jk(x-nD)}$ and $P_{n+1}^-(x) = C_{n+1}^- e^{jk(x-nD)}$. Combining the continuity of sound pressure and volume velocity at the point $x = nD$ yields the relation between the nth cell and $n^{\text{th}}+1$ cell in the form of matrix, called the periodic transfer matrix[28] $\mathbf{T}$, as

$$\begin{bmatrix} C_{n+1}^+ \\ C_{n+1}^- \end{bmatrix} = \mathbf{T}\begin{bmatrix} C_n^+ \\ C_n^- \end{bmatrix} \tag{26}$$

where the 2×2-dimensional matrix $\mathbf{T}$ is given by

$$\mathbf{T} = \begin{bmatrix} \left(1 - \frac{1}{2}\frac{S_1}{S_d}\frac{\rho c}{Z_b}\right)e^{-jkD} & -\frac{1}{2}\frac{S_1}{S_d}\frac{\rho c}{Z_b}e^{jkD} \\ \frac{1}{2}\frac{S_1}{S_d}\frac{\rho c}{Z_b}e^{-jkD} & \left(1 + \frac{1}{2}\frac{S_1}{S_d}\frac{\rho c}{Z_b}\right)e^{jkD} \end{bmatrix}. \tag{27}$$

The entry in the ith row and the jth column of $\mathbf{T}$ is denoted as t_{ij}, and Z_b is the acoustic characteristic impedance of the resonator in the neck opening, as $Z_b = P_1/V_1|_{z_1=0}$, where P_1 and V_1 are described in Eqs. (1) and (2).

Dynamic periodic systems are unlike static periodic systems, which can be described in terms of a periodic function $f(x)$, with the relation $f(x+L) = f(x)$, where L is the periodicity of the function. Instead, dynamic periodic systems (such as the structure considered in this section) can be described by the function $f(x+L) = e^{\mu}f(x)$. This is called the Bloch wave theory.[11] Therefore, Eq. (26) can be rewritten in another form, as

$$\begin{bmatrix} C_{n+1}^+ & C_{n+1}^- \end{bmatrix}^T = e^{\mu}\begin{bmatrix} C_n^+ & C_n^- \end{bmatrix}^T. \tag{28}$$

Combining Eqs. (26) and (28), the analysis of a periodic resonator system boils down to an eigenvalue problem that involves finding the eigenvalue $\lambda = e^{\mu}$ and the corresponding eigenvector $\mathbf{v} = [v^+ \quad v^-]^T$ for the transfer matrix $\mathbf{T}$.

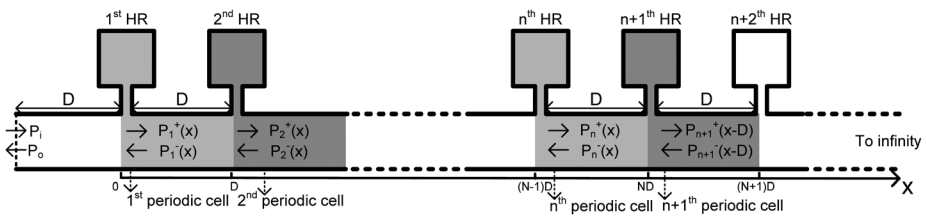

FIG. 2. Semi-infinite duct loaded periodically with resonators.

B. Nature of the characteristic wave type

μ in Eq. (28) is called the propagation constant,[5] which is a complex value composed of a real part μ_r, called the attenuation constant, and an imaginary part μ_i, called the phase constant ($\mu = \mu_r + j\mu_i$). In principle there are ranges of frequencies in which the solution contains the real part μ_r. This result indicates that the energy gets attenuated when waves travel through each periodic cell, and those frequency ranges are called the stop bands. In other frequency ranges, the solution only contains the imaginary part μ_i, which indicates that there is only a phase delay when a wave travels through each cell. These frequency ranges that the waves are allowed to propagate through are called the pass bands.

Combining Eqs. (26) and (28) yields the characteristic polynomial[29] of $\mathbf{T}$. Note that—for a passive system—the determinant of the matrix $\mathbf{T}$ is unity[28] and

$$e^{2\mu} - (t_{11} + t_{22})e^{\mu} + t_{11}t_{22} - t_{12}t_{21} = e^{2\mu} - (t_{11} + t_{22})e^{\mu} + 1 = 0. \tag{29}$$

Consequently, we can write

$$\cos(j\mu) = \frac{1}{2}(t_{11} + t_{22}) = \frac{1}{2}\left((e^{jkD} + e^{-jkD}) + \frac{1}{2}\frac{S_1}{S_d}\frac{\rho c}{Z_b}(e^{jkD} - e^{-jkD})\right). \tag{30}$$

Equation (30) indicates that μ is a function of the frequency and other geometric parameters, such as periodic distance (D) and resonator acoustic characteristic impedance (Z_b). In general, the eigenvalue $\lambda = e^{\mu}$ describes the propagation property of a characteristic wave type, and the characteristic wave type is defined by its corresponding eigenvalue $[v^+ \quad v^-]^T$, which represents the specific linear combination of positive- and negative-going planar waves. There are two solutions of μ in Eq. (30) that occur in opposite pairs: $\mu = \pm(\mu_r + j\mu_i)$ in the stop band, and $\mu = \pm j\mu_i$ in the pass band. Assumed that $\mu_r > 0$ and $0 \le \mu_i < 2\pi$, $\mu_1 = -(\mu_r + j\mu_i)$ describes the propagation property of the "positive-going" characteristic wave type (or simply positive wave type), defined by the corresponding eigenvector $\mathbf{v}_1 = [v_1^+ \quad v_1^-]^T$. Similarly, $\mu_2 = \mu_r + j\mu_i$ describes the propagation property of the "negative-going" characteristic wave type (or simply negative wave type), defined by the corresponding eigenvector $\mathbf{v}_2 = [v_2^+ \quad v_2^-]^T$. It can be imaged that these two wave type are of the same characteristic wave type but traveling in opposite directions, and there are relations between two corresponding eigenvectors ($\mathbf{v}_1 = [v_1^+ \quad v_1^-]^T$ and $\mathbf{v}_2 = [v_2^+ \quad v_2^-]^T$), as $|v_1^+| = |v_2^-|$, and $|v_1^-| = |v_2^+|$.

When planar waves travel in the semi-infinite duct with periodic resonators considered in this section, only the positive-going characteristic wave type $\mathbf{v}_1$ exists in duct segments of all periodic cells, as

$$\begin{bmatrix} C_n^+ \\ C_n^- \end{bmatrix} = a_n\mathbf{v}_1 = a_n\begin{bmatrix} v_1^+ \\ v_1^- \end{bmatrix}, \quad n = 1, 2, \ldots, \infty \tag{31}$$

where a_n is a complex constant. By introducing Eq. (26), Eq. (31) can be expressed as

$$\begin{bmatrix} C_n^+ \\ C_n^- \end{bmatrix} = \mathbf{T}\begin{bmatrix} C_{n-1}^+ \\ C_{n-1}^- \end{bmatrix} = \mathbf{T}^2\begin{bmatrix} C_{n-2}^+ \\ C_{n-2}^- \end{bmatrix} = \cdots = \mathbf{T}^{n-1}\begin{bmatrix} C_1^+ \\ C_1^- \end{bmatrix} = a_1\mathbf{T}^{n-1}\mathbf{v}_1 = a_1\lambda_1^{n-1}\mathbf{v}_1 \tag{32}$$

which gives $a_n = a_1\lambda_1^{n-1}$. Equation (32) indicates that the positive- and negative-going planar waves in duct segments of all periodic cells have the same amplitude ratio $|v_1^+/v_1^-|$ and decay at the same rate a_{n+1}/a_n ($=e^{-\mu_r}$) when they pass through each periodic cell along the positive-x direction. In other words, they propagate as a whole in the positive-x direction, denoted as the positive-going characteristic wave type. Let $\mu_1 = -jqD$ ($\lambda_1 = e^{-jqD}$), the sound pressure in the duct segment of nth periodic cell can be expressed as

$$P_n(x) = C_n^+e^{-jk(x-(n-1)D)} + C_n^-e^{jk(x-(n-1)D)} = [a_1v_1^+e^{-jk(x-(n-1)D)} + a_1v_1^-e^{jk(x-(n-1)D)}]e^{-jq(n-1)D}. \tag{33}$$

Let us set $x_n = x - (n-1)D$ ($0 \le x_n \le D$), which is a local variable. The exponential component of Eq. (33) ($e^{-jq(n-1)D}$) represents net changes of the characteristic wave type from cell to cell in a positive-x direction. The terms in square bracket ($a_1v_1^+e^{-jkx_n} + a_1v_1^-e^{jkx_n}$) represent components of the characteristic wave type, and its behavior in a periodic cell. Besides, Eq. (33) indicates that the positive-going characteristic wave type $\mathbf{v}_1$ contains the negative-going planer wave component v_1^-. Moreover, Eq. (33) can be expressed as

$$P_n(x) = [a_1v_1^+e^{-j(k-q)x_n} + a_1v_1^-e^{j(k+q)x_n}]e^{-jqx} = \Phi_1(x_n)e^{-jqx}. \tag{34}$$

It can be noted that the x in the exponential term e^{-jqx} is a global variable, Eq. (34) describes the sound pressure distribution in the whole duct. This is another expression of the positive-going characteristic wave type. It can be seen that q is the wave number of the wave type.

Figure 3 shows the dispersion of the attenuation constant μ_r, in terms of $20\log_{10}(e^{\mu_r})$, and the phase constant μ_i.

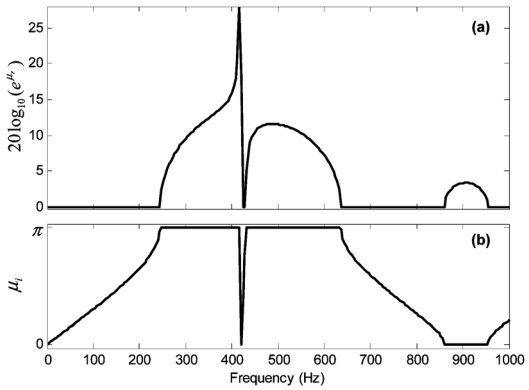

FIG. 3. Frequency variation of the real and imaginary parts of the propagation constant for the positive-going characteristic wave type in the semi-infinite duct with periodic resonators.

Resonators, with neck radius $r_1 = 1.7$ cm, length $l_1 = 4.55$ cm and cavity radius $r_2 = 4.7$ cm, length $l_2 = 4$ cm, mounted on a duct of cross sectional area $S_d = 13.2$ cm^2 is selected here, with periodic distance $D = 40$ cm. The positive-going characteristic wave type is seen to propagate without attenuation over the two broad bands of 0–240 Hz and 630–870 Hz with a phase change per cell μ_i. A strong stop band is found in the frequency range of 240–630 Hz, with a phase inversion between two nearby periodic cells (i.e., $\mu_i = \pi$). It should be noted that there is a sharp gap at around 425 Hz in the stop band, which belongs to the phase inverse of a single resonator at its resonant frequency f_0. Basically, the frequency positions of the peak and gap of the stop band are related to the f_0 of the single resonator, the bandwidth of which is controlled by the periodic distant D, as well as the geometries of both duct and resonators. The dispersion of the frequency band into the stop and pass bands is due to wave coupling, which is similar to the waves that Yun and Mak[10] observed propagating in a periodic structure.

Figure 4 shows the ratio of negative- and positive-going planar wave components in the positive-going characteristic wave type in terms of $|v_1^-/v_1^+|$, ignoring the phase difference between them. The dimensions of duct, resonators and periodic distance used here maintain the same as those used in Fig. 3, so the stop and the pass bands are the same as shown in Fig. 3(a). It can be seen that even in the pass bands of the positive-going characteristic wave type as shown in Fig. 3(a), a small amount of negative-going planar wave component v_1^- exists, which means the "pass band" is fully passed for the characteristic wave type, but not for the planar waves. In the situation of planar waves traveling through a single resonator, a full reflection only occurs at the resonance frequency f_0 of the resonator. In contrast, a full reflection (i.e., $|v_1^-/v_1^+| = 1$) is observed here in the whole stop band (240–630 Hz and 870–940 Hz) regardless of whether the characteristic wave type decays significantly or only slightly.

C. Response of a semi-infinite duct loaded periodically with resonators

This study also investigated a semi-infinite duct with periodic resonators responding to external excitation, which is a positive-going sound wave of pressure magnitude $P_i = 1$. This can be described by the maximum sound pressure in the duct segments of the first five periodic cells. The maximum sound pressure in the duct segment of the nth cell $P_{n,\max}$ can be calculated by finding the maximum[30] of

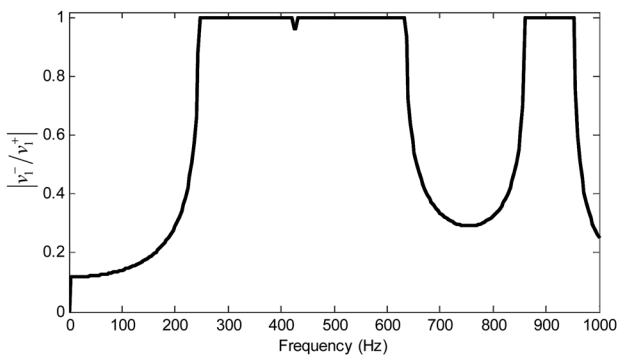

FIG. 4. Frequency variation of the positive- and negative-going planar wave components of the positive-going characteristic wave type in the semi-infinite duct with periodic resonators.

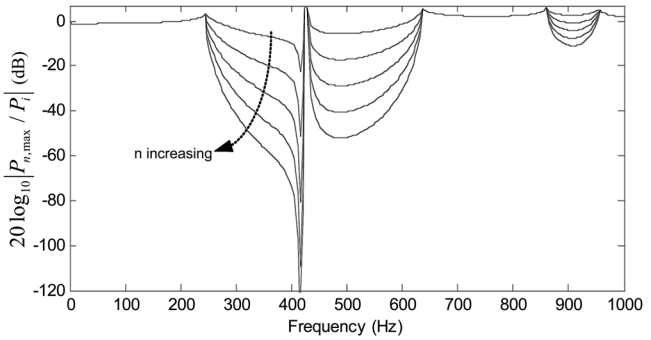

FIG. 5. Frequency variation of the maximum sound pressure in duct segments of the first five periodic cells of the semi-infinite structure, $n = 1, 2 \ldots 5$.

$$P_n(x) = P_n^+(x) + P_n^-(x) = C_n^+ e^{-jk(x-(n-1)D)} + C_n^- e^{jk(x-(n-1)D)}, \quad n = 1, 2, \ldots, 5. \tag{35}$$

The dimensions of the duct, resonators and periodic distance used in Fig. 5 maintain the same as those used in Fig. 3. Figure 5 clearly shows the occurrence of the pass bands and stop bands that are associated with the corresponding propagation constant in Fig. 3(a). In the main stop band of 240–630 Hz, the energy of the propagating waves drops at a rate of about 10 dB per periodic cell. It is also seen that the system has a strong attenuation peak at the natural frequency of a single resonator (i.e., around 415 Hz).

IV. WAVE PROPAGATION IN A FINITE-LENGTH DUCT LOADED PERIODICALLY WITH *N* RESONATORS

A. Theoretical outline

In the previous section, for a semi-infinite duct with periodic resonators, there is only the positive-going characteristic wave type defined by the eigenvector $\mathbf{v}_1$. This section considers a more general situation: a finite-length duct with N periodic resonators. In this case, the influence of the end boundary condition should be considered. This means in addition to the positive-going characteristic wave type, the negative one defined by the eigenvector $\mathbf{v}_2$ needs to be considered, which can be regarded as the "reflected" characteristic wave type.

Figure 6 shows a duct loaded periodically with N side-branch resonators at an identical distance D between two nearby resonators. At the beginning of the duct there is a loudspeaker that oscillates at the magnitude of sound pressure P_0 at the distance L_{begin} from the first resonator. At the end of the duct there is a material with reflection coefficient α at the distance L_{end} from the Nth resonator.

Similar to Sec. III, the sound pressure in the duct segment of the nth periodic cell can be described as $P_n(x) = C_n^+ e^{-jk(x-(n-1)D)} + C_n^- e^{jk(x-(n-1)D)}$, in which the magnitude of positive- and negative-going planar waves can be

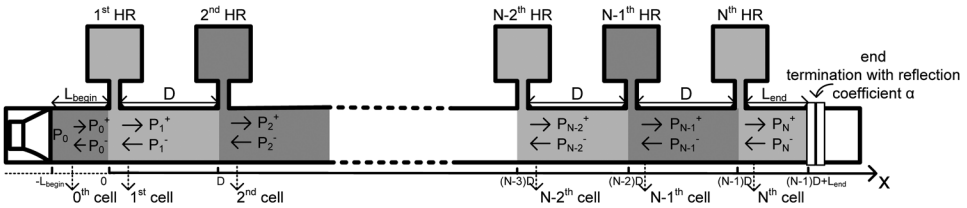

FIG. 6. Finite-length duct loaded periodically with N resonators.

obtained by adding the part of negative-going characteristic wave type $\mathbf{v}_2$ into Eq. (31), as

$$\begin{bmatrix} C_n^+ \\ C_n^- \end{bmatrix} = a_n \mathbf{v}_1 + b_n \mathbf{v}_2 = a_n \begin{bmatrix} v_1^+ \\ v_1^- \end{bmatrix} + b_n \begin{bmatrix} v_2^+ \\ v_2^- \end{bmatrix} \tag{36}$$

where b_n is also a complex constant. By introducing Eq. (26), Eq. (36) also can be expressed as

$$\begin{aligned} \begin{bmatrix} C_n^+ \\ C_n^- \end{bmatrix} &= \mathbf{T} \begin{bmatrix} C_{n-1}^+ \\ C_{n-1}^- \end{bmatrix} = \mathbf{T}^2 \begin{bmatrix} C_{n-2}^+ \\ C_{n-2}^- \end{bmatrix} = \ldots = \mathbf{T}^{n-1} \begin{bmatrix} C_1^+ \\ C_1^- \end{bmatrix} \\ &= a_1 \mathbf{T}^{n-1} \mathbf{v}_1 + b_1 \mathbf{T}^{n-1} \mathbf{v}_2 = a_1 \lambda_1^{n-1} \mathbf{v}_1 + b_1 \lambda_2^{n-1} \mathbf{v}_2. \end{aligned} \tag{37}$$

Combining Eqs. (36) and (37) gives $a_n = a_1 \lambda_1^{n-1}$ and $b_n = b_1 \lambda_2^{n-1}$.

The periodic function in the Nth cell (as shown in Fig. 6) is also valid in the range $(N-1)D \le x \le (N-1)D + L_{end}$ by assuming that the cell is also "length" D, but the sound pressure in $x = (N-1)D + L_{end}$ matches the end boundary condition, as

$$\begin{aligned} \left. \frac{P_N^-(x)}{P_N^+(x)} \right|_{x=(N-1)D+L_{end}} &= \left. \frac{C_N^- e^{jk(x-(N-1)D)}}{C_N^+ e^{-jk(x-(N-1)D)}} \right|_{x=(N-1)D+L_{end}} \\ &= \frac{a_1 \lambda_1^{N-1} v_1^- e^{jkL_{end}} + b_1 \lambda_2^{N-1} v_2^- e^{jkL_{end}}}{a_1 \lambda_1^{N-1} v_1^+ e^{-jkL_{end}} + b_1 \lambda_2^{N-1} v_2^+ e^{-jkL_{end}}} \\ &= \alpha. \end{aligned} \tag{38}$$

Similarly, the periodic function in the 0th cell (as shown in Fig. 6) is also valid in the range $-L_{begin} \le x \le 0$ by assuming that the cell is also "length" D, but the sound pressure in $x = -L_{begin}$ matches the beginning boundary condition, as

$$\begin{aligned} P_0^+(x) + P_0^-(x)\big|_{x=-L_{begin}} &= C_0^+ e^{-jk(x+D)} + C_0^- e^{jk(x+D)}\big|_{x=-L_{begin}} \\ &= (a_1 \lambda_1^{-1} v_1^+ + b_1 \lambda_2^{-1} v_2^+) e^{-jk(D-L_{begin})} \\ &\quad + (a_1 \lambda_1^{-1} v_1^- + b_1 \lambda_2^{-1} v_2^-) e^{jk(D-L_{begin})} \\ &= P_0. \end{aligned} \tag{39}$$

So the complex constants a_1 and b_1 can be solved by combining the boundary conditions [Eqs. (38) and (39)], which means for a certain beginning- and end-boundary condition, the sound pressure in the duct segment of the nth periodic cell can be described by the specific combination of the positive- and negative-going characteristic wave types, as $a_1 \lambda_1^{n-1} \mathbf{v_1} + b_1 \lambda_2^{n-1} \mathbf{v_2}$.

General speaking, in the finite-length duct with N periodic resonators, the positive-going planar waves can be divided into two parts (i.e., $C_n^+ = a_n v_1^+ + b_n v_2^+$), the first part $a_n v_1^+$ decays at the rate a_{n+1}/a_n $(=\lambda_1)$ with the other part $b_n v_2^+$ increasing at the rate b_{n+1}/b_n $(=\lambda_2)$. Due to the relation $\lambda_1 = 1/\lambda_2$ discussed in previous section, these two parts actually decay at the same rate but in opposite directions: one $a_n v_1^+$ as a component of the positive-going characteristic wave type with the other $b_n v_2^+$ belonging to the negative-going characteristic wave type. Similarly, the negative-going planar waves can also be divided into two parts (i.e., $C_n^- = a_n v_1^- + b_n v_2^-$), with one $a_n v_1^-$ moving forward and the other $b_n v_2^-$ backward. Similar to Eq. (34), the sound pressure field in the whole duct can be expressed as $P_n(x) = \Phi_1(x_n) e^{-jqx} + \Phi_2(x_n) e^{jqx}$, where $\Phi_2 = b_1 v_2^+ e^{-j(k-q)x_n} + b_1 v_2^- e^{j(k+q)x_n}$ represents the components of the negative-going characteristic wave type.

B. A finite-length duct-resonator structure with anechoic termination

Although the positive- and negative-going characteristic wave types belong to the same characteristic wave type, they propagate in opposite directions along the duct. Their relative ratio in the duct segment of the nth periodic cell can be expressed as $\delta_n = |b_n/a_n|$ $(0 \le n \le N)$.

Under the condition of a semi-infinite duct with periodic resonators, there is no negative-going characteristic wave type (i.e., $\delta_n = 0$). In contrast, δ_n is a function of frequency in a finite-length duct with N periodic resonators. Figure 7 shows the variation of δ_n under anechoic termination in a finite-length duct with ten resonators (N = 10). The dimensions of duct, resonators and periodic distance used here maintain the same as those used in Fig. 3, so the stop and the pass bands are the same as shown in Fig. 3(a). It should be noted that although Fig. 3 only shows the stop and the pass bands of the positive-going characteristic wave type, it can be imaged that the negative one has the same frequency band dispersion since they are of the same characteristic

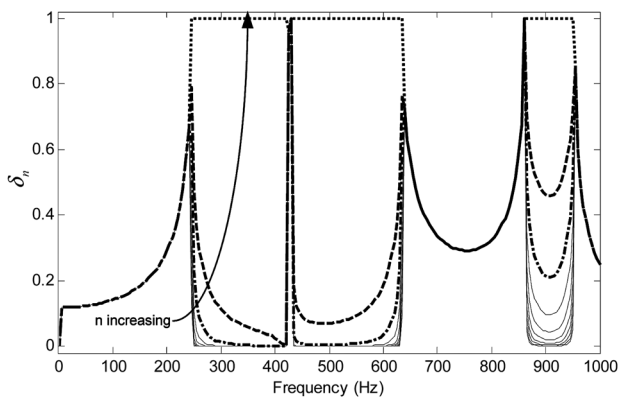

FIG. 7. Frequency variation of the finite periodic structure under anechoic termination, $n = 0, 1, \ldots, 10$.

wave type. In the stop bands (240–630 Hz and 870–940 Hz), there are few waves of the negative wave type in the duct segment of the first periodic cell ($\delta_n = 0$). In addition, it can be seen in the stop bands that the amount of the negative wave type continues to increase in the subsequent periodic cells, and finally reaches the same amount as the positive one ($\delta_n = 1$) in the last periodic cell (the Nth cell). In other words, δ_n reaches its minimum value at the beginning ($n = 0$) and its maximum value at the end ($n = 10$). It is interesting to see that even though "anechoic termination" does not reflect any planar waves, it is an absolutely "rigid" termination for the characteristic wave type in the stop bands, since it fully reflects the positive wave type in the Nth cell, as the dotted line in Fig. 7 shows.

In the pass bands (0–240 Hz, 630–870 Hz, and above 940 Hz), it can be seen that all the lines overlap. This means that the relative ratio of the positive- and negative-going characteristic wave types (δ_n) has the same pattern in all periodic cells, as both the positive- and negative-going characteristic wave types propagate freely without any attenuation in the duct. In the pass bands, the "anechoic termination" seems to be a partially reflective boundary for the characteristic wave type.

It should be noted that the amount of negative wave type quickly increases at the pass band and stop band junctures, at frequencies around 240, 430, 640, 870, and 940 Hz in all periodic cells. The system seems to respond strongly at these frequencies. It is more prominent in the gap of the stop band, i.e., a sharp boundary at around 425 Hz [as shown in Fig. 3(a)], because the characteristic wave type is fully reflected and the amount of negative wave type is nearly the same as that of the positive one. In general, unlike what it means to planar waves, anechoic termination cannot be regarded as "anechoic" to the characteristic wave type, and it can even be fully reflective at a particular frequency.

C. Estimating the properties of the characteristic wave type in an N-cell duct-resonator structure with anechoic termination

First of all, δ_N can be used to estimate the ratio of $|v_1^-/v_1^+|$ described in Sec. III by rewriting Eq. (38) under anechoic termination as

$$a_1\lambda_1^{N-1}v_1^- e^{jkL_{end}} + b_1\lambda_2^{N-1}v_2^- e^{jkL_{end}} = a_N v_1^- e^{jkL_{end}} + b_N v_2^- e^{jkL_{end}} = 0. \tag{40}$$

So there is

$$|\delta_N| = \left|\frac{b_N}{a_N}\right| = \left|\frac{v_1^-}{v_2^-}\right| = \left|\frac{v_1^-}{v_1^+}\right| \tag{41}$$

by using the relation $|v_1^+| = |v_2^-|$, which was discussed in Sec. III. This can be verified by comparing Fig. 4 and the dotted line in Fig. 7.

Furthermore, the averaged transmission loss $\overline{TL}$ of this finite-length duct with N periodic resonators can be used to estimate the attenuation constant μ_r in terms of $20\log_{10}(e^{\mu_r})$. The averaged transmission loss $\overline{TL}$ can be expressed as

$$\overline{TL} = \frac{20}{N}\log_{10}\left|\frac{P_0^+}{P_N^+}\right| = \frac{20}{N}\log_{10}\left|\frac{C_0^+}{C_N^+}\right| = \frac{20}{N}\log_{10}\left|\frac{a_1\lambda_1^{-1}v_1^+ + b_1\lambda_2^{-1}v_2^+}{a_1\lambda_1^{N-1}v_1^+ + b_1\lambda_2^{N-1}v_2^+}\right| = \frac{20}{N}\log_{10}|\mathrm{X}|. \tag{42}$$

Within the frequency range of stop bands, there is

$$\lambda_1 = e^{-\mu_r - j\mu_i}, \lambda_2 = e^{\mu_r + j\mu_i}, \quad \mu_r > 0 \quad \text{and} \quad 0 \le \mu_i < 2\pi. \tag{43}$$

Because $|\lambda_1| < 1$, when $N \to \infty$, the first term in Eq. (40) approaches zero, so $b_1 = 0$. Therefore, Eq. (42) can be rewritten as

$$\overline{TL} = \frac{20}{N}\log_{10}\left|\frac{a_1\lambda_1^{-1}v_1^+}{a_1\lambda_1^{N-1}v_1^+}\right| = 20\log_{10}(e^{\mu_r}). \tag{44}$$

Within the frequency range of pass bands, there is

$$\lambda_1 = e^{-j\mu_i}, \lambda_2 = e^{j\mu_i}(0 \le \mu_i < 2\pi) \tag{45}$$

and the X in the Eq. (42) can be rewritten as

$$\mathrm{X} = \frac{e^{j\mu_i}a_1v_1^+ + e^{-j\mu_i}b_1v_2^+}{e^{-j(N-1)\mu_i}a_1v_1^+ + e^{j(N-1)\mu_i}b_1v_2^+} = \frac{a_0v_1^+ + b_0v_2^+}{e^{-jN\mu_i}a_0v_1^+ + e^{jN\mu_i}b_0v_2^+} \tag{46}$$

which can be regarded as the addition of the vectors $a_0v_1^+$ and $b_0v_2^+$ divided by the addition of themselves with an $N\mu_i$ degree rotation of $a_0v_1^+$ in the clockwise direction and an $N\mu_i$ degree rotation of $b_0v_2^+$ in the counter-clockwise direction. By substituting Eq. (46) into Eq. (42), $\overline{TL}$ fluctuates over the pass band since the phase constant μ_i is the function of frequency. On the other hand, $\overline{TL}$ decreases at the rate of 1/N and the fluctuation of $\overline{TL}$ becomes smaller when the number of periodic cells (N) increases. Moreover, $\overline{TL}$ approaches zero [i.e., is close to $20\log_{10}(e^{\mu_r})$] within the pass band in the semi-finite duct with periodic resonators when N approaches to infinity, as shown in Fig. 3(a).

Compared with the semi-infinite duct with periodic resonators discussed in Sec. III, this section investigates two cases: two ducts with three and ten resonators, respectively, under anechoic termination, as shown in Fig. 8. It is noted that the case N = 1 is also investigated, which is the common condition that a duct with a single side-branch resonator. In addition, the attenuation constant μ_r in terms of $20\log_{10}(e^{\mu_r})$ in Fig. 3(a) is re-plotted in Fig. 8, which has been verified above that equals to $\overline{TL}$ in the case $\mathrm{N} = \infty$. The dimensions of duct, resonators and periodic distance maintain the same as those used in Fig. 3. When the case N = 1 is compared to other three cases ($N = 3$, 10 and ∞), one can have a clear impression of the difference brought by structural periodicity. In the frequency range of 150–240 Hz and 640–860 Hz, different from a single resonator ($N = 1$) providing slightly

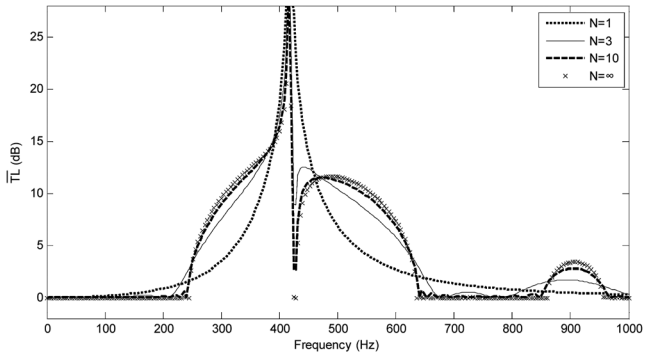

FIG. 8. Using the averaged transmission loss $\overline{TL}$ to estimate the attenuation constant μ_r in terms of $20\log_{10}(e^{\mu_r})$.

attenuation of around 0.5–2 dB, planar waves propagate without any decay through the resonators array ($N=\infty$). On the other hand, the combination of several identical resonators provides more averaged noise attenuation than the single resonator in the frequency range 240–380 Hz and 480–640 Hz of the main stop band ($N=\infty$). When the three cases of N = 3, 10 and ∞ are compared, one can see that the averaged transmission loss $\overline{TL}$ approaches the attenuation constant μ_r in terms of $20\log_{10}(e^{\mu_r})$ (i.e., the case $N=\infty$) in the stop bands as N increases. Similarly, as N increases, $\overline{TL}$ approaches $20\log_{10}(e^{\mu_r})$ with the ripple pattern of $\overline{TL}$ decreasing in both cases of $N=3$ and 10 in the pass bands.

V. NUMERICAL SIMULATION BASED ON THE FINITE ELEMENT METHOD

A three-dimensional finite element method was used to verify the theoretical analysis of the finite-length duct with periodic resonators discussed in Sec. IV; it is then compared with the experimental results in Sec. VI. The detailed description of this method for time-harmonic acoustics in this paper, which are governed by the Helmholtz equation, can be found in numerous sources.[31] The numerical model consisted of a duct with five identical side-branch resonators ($N=5$) and an excitation from an oscillating sound pressure at fixed magnitude $P_0=1$. The dimensions of duct, resonators and periodic distance used here maintained the same as those used in Fig. 3. The end termination was set to be anechoic (i.e., $\partial P/\partial x + jkP = 0$).[32] To ensure accuracy, a fine mesh spacing of less than 5 cm was maintained for the models. The mesh divided it into more than 8000 triangular elements. The maximum element was observed in the duct with a side length of 4.8 cm; the minimum element was observed in the neck-duct interface with a side length of 1.7 mm. In order to investigate the noise attenuation effect formed by the wave coupling in the periodic duct instead of the resonance of a single resonator (415 Hz), sound field distribution (pressure magnitude) on the sliced plane along the duct were examined at 500 Hz. It can be seen from Fig. 9 that sound pressure dropped noticeably at a rate of around 10 dB per cell.

VI. EXPERIMENT

Figure 10 shows the experimental setup for the measurement of the sound pressure in a duct with an array of resonators. Similar to the numerical model, the experimental apparatus consisted of a duct with five identical side-branch resonators and a loudspeaker mounted at the beginning. In the experiment, two replaceable end terminations were used. One is rigid end termination and one is a termination with absorptive materials. The transfer matrix method was used.[33,34] This method including the two-microphone technique is used to separate incident and reflected waves for calculation of the transmission loss by placing one pair of microphones before and another pair after the resonators array, and the two-load method to yield strict anechoic end termination. A detailed description of the transfer matrix method can be found in Ref. 33. The testing apparatus consisted of four B&K 1/4" type 4935 microphones, a B&K PULSE analyzer with four input channels and two output channels, and a B&K type 2706 power amplifier. The mismatches of the four microphones were carefully calibrated following Ref. 34. The calculated transmission loss is then divided by the number of resonators (N = 5) as averaged transmission loss $\overline{TL}$, that can be regarded as an approximation of the attenuation constant μ_r in terms of $20\log_{10}(e^{\mu_r})$, as discussed in Sec. IV. The dimensions of duct, resonators are the same as that discussed in the previous sections, except now $l_1 = 5$ cm and $D = 47$ cm. These dimensions of the duct and resonators are similar to that in Ref. 19, which are selected to investigate nonplanar waves excited in the resonators neck-cavity interface and to ensure planar wave propagation in the duct and neck with higher-mode waves decay quickly.

VII. RESULTS AND DISCUSSION

Figure 11 shows the comparison of the average transmission loss $\overline{TL}$ between the experiment, the theory using

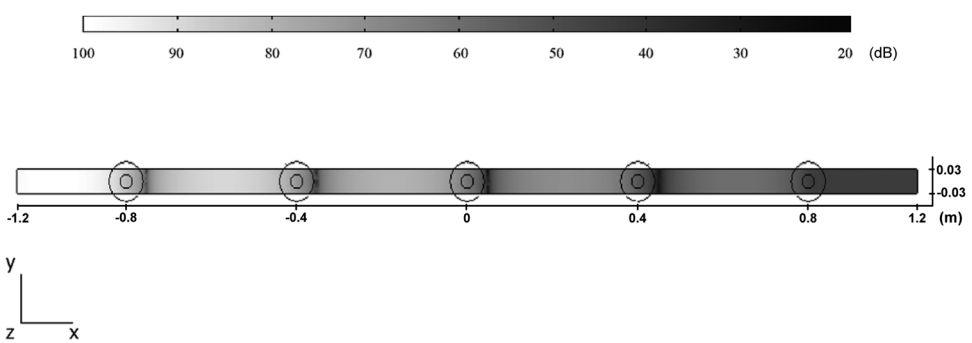

FIG. 9. Sound field (pressure magnitude) of the finite periodic structure.

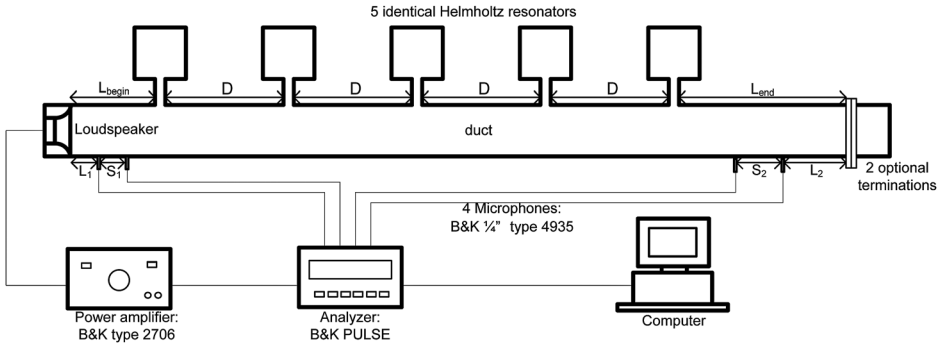

FIG. 10. The experimental setup for measurement.

the distributed-parameter model, and the FEM simulation for a duct with five identical side-branch resonators. It can be seen from Fig. 11 that the changes in the geometry of the structure result in the difference of the range of the main stop band, the position of the gap, and the peak of the main stop band compared to Fig. 8. As shown in Fig. 11, the FEM simulation fits better with the experimental data than the theoretical predictions both in the stop bands and in the ripple of the pass bands. The deviation of the experiment data from other two methods at the sharp peak is probably due to the sensitivity of the microphones, which is similar to that observed in Ref. 14. However, instead of the sharp peak resulted from the resonance of a single resonator, the broad noise attenuation band from 210 to 570 Hz is a more important feature for this periodic structure because it can provide considerable noise attenuation in both magnitude and bandwidth. It can be seen from Fig. 11 that the averaged transmission loss $\overline{TL}$ in the main stop band is about 3–15 dB, except the narrow gap at around 380 Hz and the sharp peak at around 400 Hz. In this finite-length duct with five identical resonators (i.e., $N = 5$), the overall transmission loss TL is about 15–75 dB (i.e., 5×3–15 dB) in the stop band except the gap and the peak. The narrow gap at around 380 Hz is being investigated. It seems that this gap can be eliminated when this periodic structure has a slight irregularity. In other words, the periodic distance D and/or the geometry of a single resonator element are not exactly identical. Future research is needed to examine this.

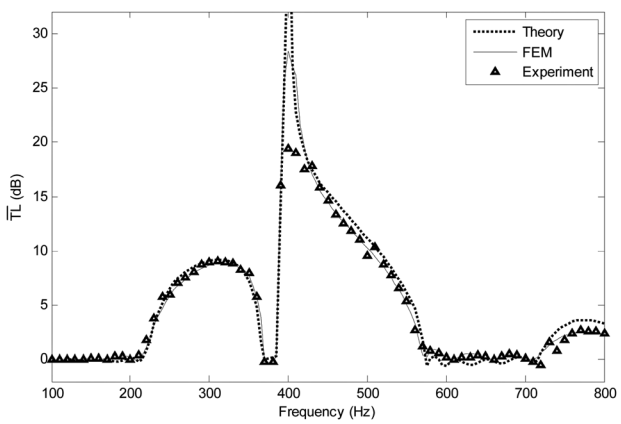

FIG. 11. A comparison of $\overline{TL}$ between experiment, the theory using distributed-parameter model and the FEM simulation for a duct loaded periodically with five identical resonators.

VIII. CONCLUSIONS

This paper has presented a theoretical study of a periodic resonators array based on the distributed-parameter resonator model. When waves travel through each resonator, they produce reflected and transmitted waves. Those reflected and transmitted waves are then reflected and transmitted again by the previous and next resonators. This process is physically repeated in the periodic structure. In this situation, instead of dividing the sound pressure field in the duct simply into positive- and negative-going planar waves, it is more appropriate to decompose it into positive- and negative-going characteristic wave types.

After introducing the characteristic wave type to describe the wave coupling in the periodic structure, both the semi-infinite duct with infinite periodic resonators and the finite-length duct with N periodic resonators have been discussed. The predicted results using this theory fit well with the FEM simulation and the experimental results. This study indicates that the use of periodic resonators may provide a much broader band of sound attenuation compared to a single resonator. It is hoped that the present study can provide a basis for investigating its potential application in noise control.

[1]D. J. Mead, "A general theory of harmonic wave propagation in linear periodic system with multiple coupling," J. Sound Vib. **27**(2), 235–260 (1973).
[2]C. E. Bradley, "Acoustic Bloch wave propagation in a periodic waveguide," Technical Report of Applied Research Laboratories, Report No. ARL-TR-91-19 (July), The University of Texas at Austin (1991).
[3]J. W. S. Rayleigh, "On the maintenance of vibrations by forces of double frequency, and on the propagation of waves through a medium endowed with a periodic structure," Philos. Mag. **XXIV**, 145–159 (1887).
[4]M. Heckl, "Investigations on the vibrations of grillages and other simple beam structures," J. Acoust. Soc. Am. **36**, 1335–1343 (1964).
[5]D. J. Mead, "Free wave propagation in periodically supported infinite beams," J. Sound Vib. **11**, 181–197 (1970).
[6]G. S. Gupta, "Natural flexural waves and the normal modes of periodically supported beams and plates," J. Sound Vib. **13**, 89–101 (1970).
[7]B. R. Mace, "Periodically stiffened fluid loaded plates II: response to line and point forces," J. Sound Vib. **73**, 487–504 (1980).
[8]D. J. Mead and N. S. Bardell, "Free vibration of a thin cylindrical shell with discrete axial stiffeners," J. Sound Vib. **111**, 229–250 (1986).
[9]D. J. Mead and N. S. Bardell, "Free vibration of a thin cylindrical shell with periodic circumferential stiffeners," J. Sound Vib. **115**, 499–520 (1987).
[10]Y. Yun and C. M. Mak, "A study of coupled flexural-longitudinal wave motion in a periodic dual-beam structure with transverse connection," J. Acoust. Soc. Am. **126**(1), 114–121 (2009).
[11]C. Kittel, *Introduction to Solid State Physics*, 6th ed. (Wiley, New York, 1986), Chap. 8, pp. 181–216.
[12]Z. Y. Tao, W. Y. He, and X. L. Wang, "Resonance-induced band gaps in a periodic waveguide," J. Sound Vib. **313**, 830–840 (2008).

[13]Y. T. Duan, W. Koch, C. M. Linton, and M. Mciver, "Complex resonances and trapped modes in ducted domains," J. Fluid Mech. **571**, 119–147 (2007).
[14]N. Fang, D. J. Xi, J. Y. Xu, M. Ambati, W. Srituravanich, C. Sun, and X. Zhang, "Ultrasonic metamaterials with negative modulus," Nature Mater. **5**, 452–456 (2006).
[15]J. W. S. Rayleigh, *The Theory of Sound, Volume II* (Dover, New York, 1945), Chap. 16, pp. 303–322.
[16]P. K. Tang and W. A. Sirignano, "Theory of a generalized Helmholtz resonator," J. Sound Vib. **26**, 247–262 (1973).
[17]P. A. Monkewitz and N. M. Nguyen-Vo, "The response of Helmholtz resonators to external excitation. Part 1. Single resonators," J. Fluid Mech. **151**, 477–497 (1985).
[18]A. Selamet and N. S. Dickey, "Theoretical, computational and experimental investigation of Helmholtz resonators with fixed volume: lumped versus distributed analysis," J. Sound Vib. **187**(2), 358–367 (1995).
[19]A. Selamet, P. M. Radavich, N. S. Dickey, and J. M. Novak, "Circular concentric Helmholtz resonator," J. Acoust. Soc. Am. **101**, 41–51 (1997).
[20]A. Trochidis, "Sound transmission in a duct with an array of lined resonators," J. Vib. Acoust. **113**, 245–249 (1991).
[21]K. T. Chen, Y. H. Chen, K. Y. Lin, and C. C. Weng, "The improvement of the transmission loss of a duct by adding Helmholtz resonators," Appl. Acoust. **57**, 71–82 (1998).
[22]S. H. Seo and Y. H. Kim, "Silencer design by using array resonators for low-frequency band nose reduction," J. Acoust. Soc. Am. **118**(4), 2332–2338 (2005).
[23]J. F. Groeneweg, "Current understanding of Helmholtz resonator arrays as duct boundary conditions," in a conference held at NASA Headquarters, Washington, DC (July 14–15, 1969), pp. 357–368 (1969).
[24]B. S. Cazzolato, C. Q. Howard, and C. H. Hansen, "Finite element analysis of an industrial reactive silencer," in *The Fifth International Congress of Sound and Vibration*, Adelaide, Australia (December 15–18, 1997), pp. 1659–1667.
[25]M. L. Munjal, *Acoustics of Ducts and Mufflers* (Wiley, New York, 1987), Chap. 1, pp. 1–39.
[26]B. G. Korenev, *Bessel Functions and their Applications* (Taylor and Francis, London, 2002), Chap. 1, pp. 7–64.
[27]J. Miles, "The reflection of sound due to a change in cross section of a circular tube," J. Acoust. Soc. Am. **16**, 14–19 (1944).
[28]L. Schächter, *Beam-Wave Interaction in Periodic and Quasi-Periodic Structures* (Springer, Berlin, 1997), Chap. 5, pp. 195–233.
[29]D. C. Lay, *Linear Algebra and its Applications* (Addison Wesley, New York, 1994), Chap. 6, pp. 280–287.
[30]L. Friis and M. Ohlrich, "Coupling of flexural and longitudinal wave motion in a periodic structure with asymmetrically arranged transverse beams," J. Acoust. Soc. Am. **118**(5), 3010–3020 (2005).
[31]L. L. Thompson, "A review of finite-element methods for time-harmonic acoustics," J. Acoust. Soc. Am. **119**(3), 1315–1330 (2006).
[32]C. Q. Wang and L. X. Huang, "Analysis of absorption and reflection mechanisms in a three-dimensional plate silencer," J. Sound Vib. **313**, 510–524 (2008).
[33]ASTM E 2611-09 *Standard Test Method for Measurement of Normal Incidence Sound Transmission of Acoustical Materials Based on the Transfer Matrix Method* (American Society for Testing and Materials, Philadelphia, 2009).
[34]Y. S. Choy, "Sound Induced Vibration and Duct Noise Control," Ph.D. dissertation, The Hong Kong Polytechnic University, Hong Kong, 2003.